

## The spectrum of temperature fluctuations in turbulent flow

By H. L. GRANT, B. A. HUGHES,  
W. M. VOGEL AND A. MOILLIET

Defence Research Establishment Pacific, † Victoria, B.C., Canada

(Received 9 September 1967 and in revised form 28 June 1968)

Temperature and velocity fluctuations have been recorded in the open sea and in a tidal channel, and power spectra have been determined from the records. The one-dimensional spectra of temperature fluctuations are found to have an inertial subrange. At larger wave-numbers the data can be fitted by Batchelor's spectrum function for the viscous-convective range. The spectra are inconsistent with the form proposed by Pao for the viscous-convective range.

Estimates are given for the constants in Batchelor's spectrum function, but these depend upon knowledge of the rate of dissipation of kinetic energy, which is determined from the velocity spectra. There is doubt about the validity of some of the velocity spectra, and in other cases there is reason to suspect that the turbulence is not locally isotropic.

---

### 1. Introduction

It has been shown theoretically that, in the absence of buoyancy forces, the power spectrum of the variations of a passive scalar contaminant arising from turbulent mixing should exhibit a  $-\frac{5}{3}$  power law form with wave-number whenever the kinetic energy spectrum possesses an inertial subrange (Batchelor 1959; Obukhov 1949; Corrsin 1951). Under the assumptions of large Prandtl (or Schmidt) number and local isotropy, Batchelor (1959) theoretically deduced the form of the power spectrum of variations of this type for the complete high wave-number end of the spectrum. It was shown that the contaminant spectrum should differ in form from the energy spectrum for wave-numbers corresponding to eddies whose motion is dominated by viscosity. In this region, the contaminant spectrum should behave as (wave-number) $^{-1}$  until the spatial scales become short enough for diffusion to become dominant, resulting in an exponentially decaying behaviour. Thus:

$$\Gamma(k) = \beta_3 \chi \epsilon^{-\frac{1}{2}} k^{-\frac{5}{3}} \quad (k \ll (\epsilon/\nu^3)^{\frac{1}{2}}), \quad (1)$$

$$\Gamma(k) = -\chi \gamma^{-1} k^{-1} \exp(Dk^2 \gamma^{-1}) \quad (k \gg (\epsilon/\nu^3)^{\frac{1}{2}}), \quad (2)$$

$$\chi = 2D \int_0^{\infty} k^2 \Gamma(k) dk, \quad (3)$$

† Formerly Pacific Naval Laboratory.

for high enough Reynolds numbers, where  $\Gamma(k)$  is the three-dimensional contaminant power spectrum function,  $\beta_3$  is a universal constant,  $\chi$  is the rate of dissipation of contaminant fluctuation per unit mass,  $\epsilon$  is the rate of dissipation of kinetic energy per unit mass,  $k$  is the radian wave-number,  $\nu$  is the kinematic viscosity and  $D$  is the coefficient of molecular diffusion.  $\gamma$ , the effective average value of the least principal rate of strain, is given by  $-q^{-1}(\epsilon/\nu)^{\frac{1}{2}}$ , where Batchelor estimates  $q = 2$ .

The essential ideas on which this is based are that, over sufficiently small eddy sizes (less than or of order the Kolmogoroff length scale), the rate of strain is approximately uniform; the principal axes of strain are locally fixed in the fluid for a duration of time long (of order ten times) compared to the rate-of-strain time scale; and the triple covariance between strain rate at a point, contaminant at the same point and contaminant at a different point (separation less than the Kolmogoroff scale) is essentially equal to the product of an effective least principal strain rate and the contaminant covariance.

As in the case of velocity fluctuations, there is no known way to make direct measurements of a three-dimensional spectrum of a scalar. Gibson & Schwartz (1963) have derived the one-dimensional form of Batchelor's spectrum and it can be written

$$\psi(k_1) = \beta_1 \chi \epsilon^{-\frac{1}{2}} k_1^{-\frac{5}{2}} \quad (k_1 < k_*) \quad (4)$$

$$\psi(k_1) = 2 \sqrt{\pi} q^{\frac{3}{2}} D^{\frac{1}{2}} \nu^{\frac{3}{2}} \epsilon^{-\frac{3}{2}} \chi \left\{ \frac{\Phi[(2q)^{\frac{1}{2}} k_1/k_B]}{(2q)^{\frac{1}{2}} k_1/k_B} - \int_{(2q)^{\frac{1}{2}} k_1/k_B}^{\infty} \Phi(y) dy \right\} \quad (k_1 > k_*) \quad (5)$$

where  $\Phi(x) = (2\pi)^{-\frac{1}{2}} \exp(-\frac{1}{2}x^2)$ , and  $k_B$  is Batchelor's characteristic wave-number for the dissipation of contaminant fluctuations, given by  $k_B = (\epsilon/\nu D^2)^{\frac{1}{2}}$ . Batchelor (1959) suggests that the wave-number  $k_*$  at which (4) and (5) intersect is of the order of the Kolmogoroff wave-number  $k_s = (\epsilon/\nu^3)^{\frac{1}{4}}$ .

For values of  $(2q)^{\frac{1}{2}} k_1/k_B$  small compared with unity, (5) reduces approximately to

$$\psi(k_1) = q \nu^{\frac{1}{2}} \epsilon^{-\frac{1}{2}} \chi k_1^{-1} \quad (6)$$

The contaminant dissipation rate  $\chi$  can also be expressed in terms of the spectrum function  $\psi(k_1)$  as

$$\chi = 6D \int_0^{\infty} k_1^2 \psi(k_1) dk_1 \quad (7)$$

In a recent paper, Pao (1965) has succeeded in developing turbulent velocity and scalar spectra pertaining to the whole universal equilibrium range. His solution is based on the concept of the migration rate of a spectral element across the spectrum and subsequent dimensional reasoning. For both types of spectra he postulates that the 'cascading' rate of a spectral element (that is, the rate at which an 'eddy's' scale size is varied, presumably by local straining) is dependent only on the kinetic energy dissipation rate and the wave-number. Simple dimensional arguments then lead to the spectral forms. The energy spectrum so deduced not only fits the experimental data which were available to him, but it leads to finite velocity derivatives of all orders. The scalar spectra have a form which is everywhere similar to the velocity spectra. Nowhere does the power spectrum in log-log form rise above the  $-\frac{5}{3}$  slope, for all values of Schmidt (Prandtl) number (in contra-distinction to Batchelor (1959)).

Hence 
$$\Gamma(k) = \beta_3 \chi \epsilon^{-\frac{1}{3}} k^{-\frac{5}{3}} \exp\left(-\frac{3}{2}\beta_3 D \epsilon^{-\frac{1}{3}} k^{-\frac{4}{3}}\right). \quad (8)$$

Gibson & Schwartz (1963) have observed the temperature fluctuations behind a heated grid in a water tunnel and the conductivity fluctuations resulting from the injection of salt water at the grid. Their spectra are not inconsistent with Batchelor's theory and only marginally different from Pao's. Unfortunately the scale of their turbulence was so small that the high wave-number regions of the spectra were affected by averaging over the area of their probes and the test of the theory is not as decisive as one would like.

Nye & Brodkey (1967) have recently published spectra derived from the fluctuations of dye concentration in water. The observations were made in a pipe flow and at 36 diameters downstream of the point of dye injection their one-dimensional spectrum function is proportional to  $k^{-0.9}$  over a range of  $1\frac{1}{2}$  decades. This is close to Batchelor's prediction for their very high Schmidt number, but unfortunately the Reynolds number of the flow was too low to allow a  $k^{-\frac{5}{3}}$  region in the spectrum and, presumably because of probe size, the spectra depart from Batchelor's spectrum at the high wave-numbers. Although the work gives substantial support to the theory, the above difficulties prevented the determination of numerical constants.

Pond *et al.* (1966) have determined spectra from measurements of temperature in the atmosphere and find that, in the inertial subrange,  $\psi(k)$  is proportional to  $k^{-\frac{5}{3}}$  but the range of these spectra was not great enough to determine the constant in (4).

In 1962 the authors made measurements of the temperature microstructure occurring in both inshore and offshore waters near Vancouver Island, B.C. The following sections of the paper are concerned with a description of the measuring techniques used, a description of the experimentally determined temperature spectra and a comparison between these results and the theoretical predictions. In these experiments the Reynolds numbers were in some cases nearly a thousand times as great as those used by Gibson & Schwartz and by Nye & Brodkey, and the dissipation rates were 10 to 100 times smaller. The eddy size at which viscosity becomes important is therefore larger and probe size is a less serious problem. In spite of this it will be seen that we are unable to observe all of the interesting part of the spectrum but we are able to come to the clear conclusion that in the viscous-convective range the spectrum rises above the  $k^{-\frac{5}{3}}$  line and goes approximately as  $k^{-1}$  in agreement with Batchelor's theory. Estimates are made of the constants that appear in this theory, but the accuracy is limited because of the uncertainty in the spectra at high wave-numbers.

Companion papers (Grant, Moilliet & Vogel 1968; Fabula 1968) discuss some observed properties of ocean turbulence in terms of the general oceanographic parameters and describe the heat transfer between the water and the thin-film thermometer and the method used to determine the frequency response of the instrument.

## 2. The oceanographic situation and observational methods

The specific locale of the inshore measurements was Discovery Passage, a narrow channel lying between Vancouver and Quadra Islands ( $50^{\circ} 02' N.$ ,  $125^{\circ} 10' W.$ ). Here the tidal currents are very strong, occasionally reaching

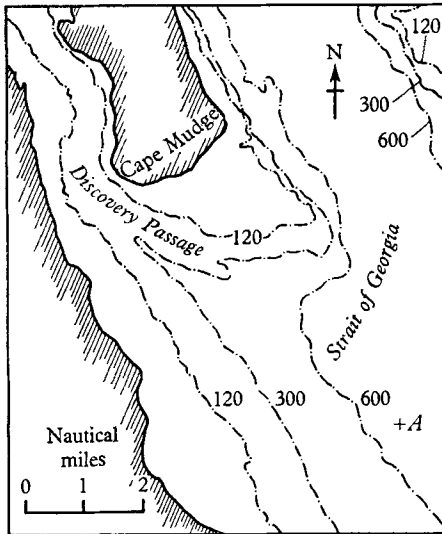


FIGURE 1

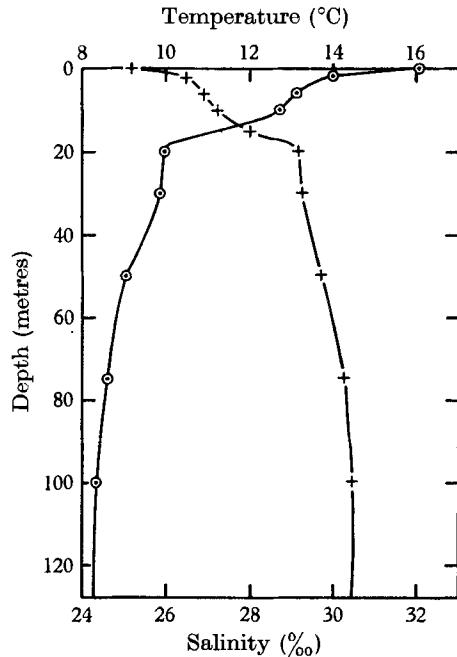


FIGURE 2

FIGURE 1. Plan of the southern entrance to Discovery Passage. The contours indicate depth in feet. In the passage, the flood tide flows from north to south.

FIGURE 2. Temperature ( $\odot$ ) and salinity ( $+$ ) structure observed at point A in figure 1.

12 knots in the narrowest part of the channel. The southern end of Discovery Passage opens into the Strait of Georgia and the northern end is connected to a series of narrow straits which extend for 160 km to the open sea. In the summer the surface water of the Strait of Georgia is affected by two important features: an excess of day-time solar heating over night-time cooling, and a large inflow of fresh water from the Fraser River. The result is a layered structure with warm, low-salinity water near the surface.

The entrance to Discovery Passage is shown in figure 1 and the temperature and salinity structure at point A is given in figure 2. On an ebb tide, this strongly layered water is drawn into the entrance of the passage, and, when it reaches the region where the depth is approximately 100 m, it breaks into violent turbulence. West of Cape Mudge the speed of the current often reaches 6 knots. At the end of a strong ebb, some temperature microstructure often appears some 20 km to the north of the area shown in figure 1 so it takes at least 6 h for the water to become thoroughly mixed.

On the early part of the flood tide the water entering Georgia Strait from the passage contains large fluctuations in temperature, but near the end of the flood it is well mixed. On this tide strong turbulence extends several miles to the south and east of the entrance, the main stream taking an almost easterly direction. Runs 1 to 4 were made in the vicinity of Cape Mudge and run 5 was made in Discovery Passage 22 km from the southern entrance. A full plan of Discovery Passage is given by Grant, Stewart & Moilliet (1962), hereafter referred to as GSM. A typical Reynolds number based on the speed of the current and the depth of the water is  $3 \times 10^8$ . In all cases, including the offshore work,  $D = 1.44 \times 10^{-3}$  cm<sup>2</sup>/sec and the value for  $\nu$  has been taken as that for fresh water at the ambient temperature. It is believed that the effect of salinity on viscosity is unimportant for the results quoted here.

The measurements in the offshore waters were obtained in the vicinity of 49° N., 127° W., about 65 km west of the coast of Vancouver Island, where the depth is about 1000 m. Observations were made at depths between 15 and 90 m.

Unfortunately, in both areas, there is considerable variation in the vertical distribution of temperature and salinity, even between observations taken only a few minutes apart. In the open sea case, the microstructure instrumentation was mounted on a submarine and the vertical structure was observed from a surface ship which had to keep about 3 km away. In the Discovery Passage area the microstructure instrumentation was towed below the surface ship and standard oceanographic observations could only be made before and after each towing period. Under these conditions it is not possible to describe the vertical structure of the water exactly at the time and place of any given run. It is possible for considerable variations to occur during the period in which a sample is being recorded because of internal waves in the ocean area and strong tidal currents in the enclosed waters.

The observations in the Discovery Passage area were made in the summer of 1962 using instruments mounted on the towed body described by GSM. For the offshore work the instrumentation was mounted on a submarine which provided a sufficiently stable platform for the measurement of small velocity fluctuations in the water. The location of the probes (Grant *et al.* 1968, figure 1) was chosen so that the effect of the hull was negligible. We currently have under development a system for towing instruments at depths down to 370 m below a surface ship in the open sea, but the motion of the towed body is not yet steady enough to permit satisfactory observation of velocity fluctuations. Brief reference is made by Grant *et al.* (1968) to some measurements of temperature fluctuations with this equipment.

Temperature fluctuations were measured with a platinum film resistance thermometer. The film which forms the sensitive element of this thermometer is about  $10^{-6}$  cm thick, and is deposited on a conically ground end of a sealed glass tube (see figure 3). Three platinum wires inside the glass tube terminate on the conical surface near the tip in separate 'spongy' platinum areas. Two of these areas are joined by two bands of deposited film, one on each side of the cone, and electrically connected in parallel. The third area makes electrical contact with

the film only by conductivity through the sea water and is used to nullify variations in apparent resistance of the film due to variations in the sea water conductivity.

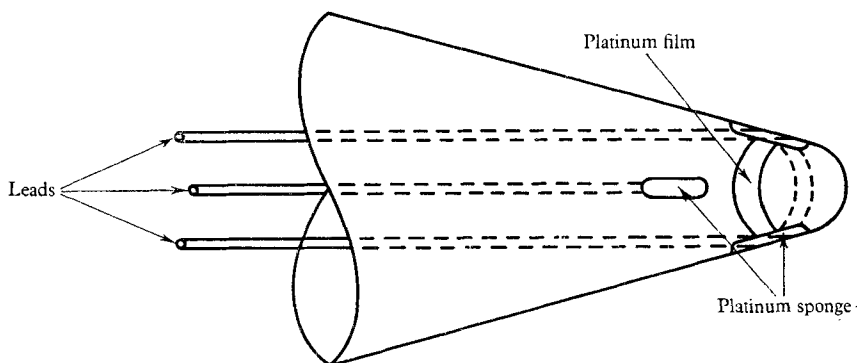


FIGURE 3. The conical tip of the thin-film resistance thermometer probe.

The film is used as one arm of an a.c. bridge circuit (see figure 4). The extra exposed electrode is connected to the bridge through compensating resistor  $R_3$ , whose value varies from probe to probe. The linear dimensions of the film are typically  $0.2 \text{ mm} \times 0.5 \text{ mm}$  for each half and it is usually deposited about  $0.5 \text{ mm}$  from the rounded tip of the cone.

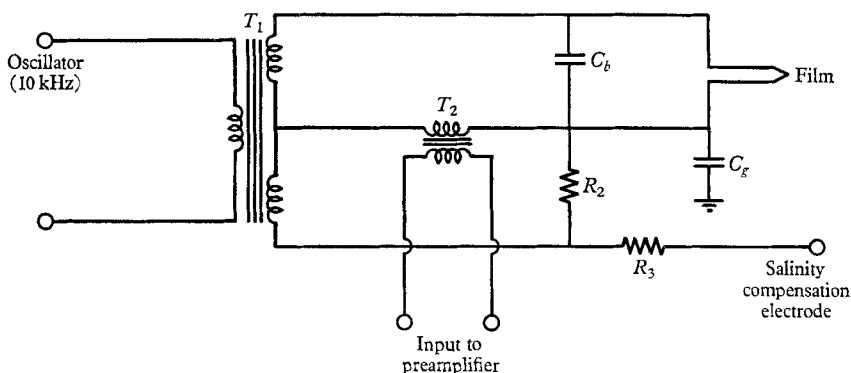


FIGURE 4. The thin-film resistance thermometer bridge.

During the towing operations, the bridge, transformers, oscillator and a pre-amplifier were located in the towed body along with similar equipment to enable simultaneous measurements of velocity microstructure. As in GSM, we found it expedient to have information available from a propellor-driven current meter, at least one thermistor, and a depth gauge—all of which were mounted on, and their respective electronics housed in, the towed body. The temperature information was transmitted to the electronics in the surface ship through two 2-conductor shielded cables 150 m long.

In order to avoid the necessity of remote-controlled bridge balance, a reference signal from the 10 kHz oscillator is transmitted to the surface ship and is used to

cancel out the signal resulting from the average unbalance of the bridge. The fluctuations about this average are fed next into an attenuator, a broad band-pass filter centred at 10 kHz (to remove undesired harmonics), an amplifier, a phase-sensitive detector and a 1.4 kHz low pass filter (figure 5). The signal, now directly representing the variation of the temperature of the platinum film about an approximate average, is connected in parallel to three d.c. amplifiers with separate gain controls. The output from one of these is put directly onto one channel of an FM tape recorder. The other two outputs are passed through differentiating amplifiers to prewhiten the spectrum of the signals and thus minimize tape recorder and subsequent analysis noise. The same equipment was used in the submarine with the bridge, oscillator and preamplifier mounted outboard near the probe.

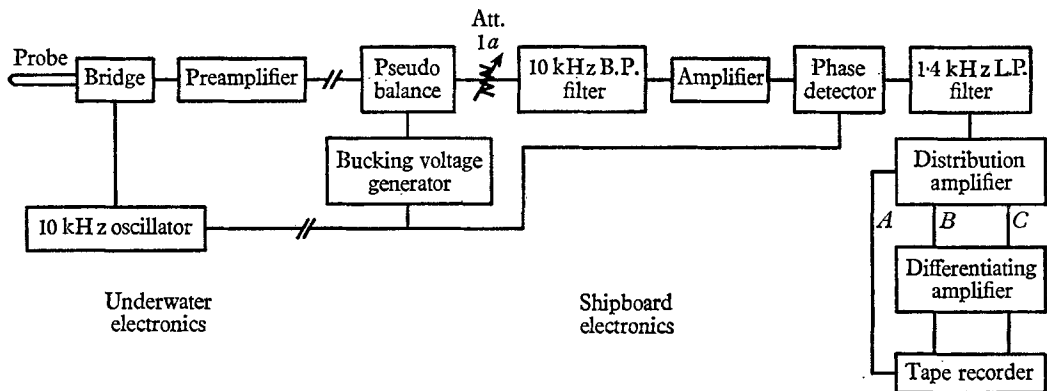


FIGURE 5. Amplifying, detecting and recording system for the thin-film resistance thermometer bridge.

In order that a system of this kind be suitable for measurement of fine scale temperature structure at sea it must satisfy certain design criteria. (i) The sensitive element must be small enough to prevent averaging over temperature structure with the smallest physical scales of interest. (ii) The frequency response must be high enough to permit recording of the highest frequencies which appear when Taylor's hypothesis is applied to these small scales. (iii) The noise level of the instrument must be suitably low over the frequency range of interest. (iv) The sensitivity to velocity and conductivity fluctuation must be low relative to the temperature sensitivity in the context of the expected variation of these quantities.

The first of these criteria has not been met in this instrument. We have simply made the probes as small as we could and the diameter is usually about 0.5 mm. This size permits the recording of signals associated with wave-numbers less than about  $100 \text{ cm}^{-1}$  which does not include all scales 'of interest'. Gibson & Schwartz (1963) encountered a similar problem, but our dissipation rates are much lower than theirs so the wave-number at which viscosity becomes important is larger. Probe size has not been the limiting factor in the present work.

The next two of these factors, frequency response and noise, together with the rapid fall-off in the temperature spectrum, determined the smallest scales or highest frequencies which could be satisfactorily recorded. The nature of the frequency response of towed conical thin-film thermometers and the methods used to determine it are discussed by Fabula (1968). It is shown there that the response is not controlled by the thermal capacity of the film, which is very small, but by the conduction of heat through the laminar boundary layer over the film. It is found that the sensitivity varies as  $\exp\{-\Delta(\pi f/D)^{\frac{1}{2}}\}$  where  $\Delta$  is approximately equal to the boundary-layer displacement thickness,  $D$  is thermal diffusivity and  $f$  is the frequency of the spectral component under examination. Fabula has devised an experimental technique for determining the effective boundary-layer thickness for each probe by towing it through a heated laminar plume.

For the particular probe used here,  $\Delta$  was determined to be  $1.86 \times 10^{-3}$  cm by a plume test for which the towing speed was 115 cm/sec and the water temperature was 18°C. Typical conditions at sea were a towing speed of 130 cm/sec and a water temperature of 10°C. It has been necessary to apply the scaling laws given by Fabula (1968, appendix) to the plume test results to determine the correct value of  $\Delta$  for each run at sea. Thus, if  $V$  is the towing speed,  $\Delta(V/\nu)^{0.32}$  is independent of Reynolds number and  $\Delta(\nu/D)^{0.30}$  is independent of Prandtl number.

The frequency above which the signal to noise ratio becomes unacceptably low depends upon the level of the signal but typical values are 100 Hz for the open sea data and 800 Hz for the strong signals from Discovery Passage.

The thermometer has some sensitivity to velocity and to the electrical conductivity of the water, which in turn is a function of both temperature and salinity. The effective thermal sensitivity is governed by two factors, the temperature coefficient of resistance of the film and the power dissipated in heat. Although higher coefficients could be obtained, we have used platinum as the film material because of its relative ease of deposition and its resistance to corrosion in sea water. Increasing the power dissipation in the film results in greater effective sensitivity because the signal strengths vary in direct proportion to the driving voltage across the probe, whereas the noise of the system is introduced in the first stage of amplification and is independent of bridge voltage. However, the velocity sensitivity is controlled by the difference in temperature between the film and the surrounding fluid, i.e. the power dissipation per unit area of film. A suitable compromise in driving voltage must then be reached. We have maintained a velocity sensitivity equivalent to about  $2.8 \times 10^{-5}$  degC/cm/sec. This has proved to be quite satisfactory for all the data reported here.

The salinity sensitivity is kept low by using a low film resistance (5 ohms) compared to the effective water-path resistance of about 200 ohms, and by compensating for variations in the water resistance by means of the previously mentioned third lead connected to an opposite phase position on the bridge. Resistor  $R_3$  in the bridge is adjusted until large steady-state changes in salinity at constant temperature and velocity are nullified. When this has been achieved it is estimated that a change in salinity of 1‰ (parts per thousand by weight) at



10 °C and 30 ‰ salinity is the equivalent of a  $2.8 \times 10^{-3}$  degC change in temperature. In the absence of simultaneous salinity fluctuation measurements, an appeal must be made to simple theoretical arguments to determine the possible source of error on this account. If the universal equilibrium theory of contaminant spectra is assumed to hold for spectral values in the inertial subrange, the ratio of the spectral levels in this range of salinity and temperature will vary as the ratio of their respective dissipation rates. In statistically steady conditions these dissipation rates will be equal to the turbulent production rates of the respective fluctuating quantities from the local mean gradients by the action of large-scale eddies. Using the concept of eddy diffusivity, and assuming equal eddy coefficients, the ratio of the dissipation rates and thus the spectral levels will be equal to the ratio of the respective mean gradients squared. Under oceanic conditions, the oceanographic data taken during the microstructure experiments indicates that the salinity varies by not more than 0.5 ‰ in a depth interval for which the temperature varies by about 1.7 degC. Thus the salinity spectral level in  $(\text{‰})^2$  per unit wave-number is about  $10^{-1}$  of the temperature spectral level in  $(\text{degC})^2$  per unit wave-number. Taking into account the square of the measured value of the equivalent salinity sensitivity of the probes, this results in an error in the measured temperature spectrum in the inertial subrange (and viscous-convective range as well) of about 1 part in  $10^6$ . For inshore waters, a similar calculation reveals that the salinity varies by less than 1 ‰ for a temperature change with depth of 1 degC. Thus in this case the error amounts to about 1 part in  $10^5$ .

We are less certain about the effect of plankton particles adhering to the probe. It can be expected that the boundary layer over the film would be thickened by the presence of a particle on the tip and that the result would be a loss of response at high frequencies. The impact of a particle on the tip of the temperature probe gives no detectable signal and even if a particle lodges on the end there is apparently no visible change in the character of the signal. Although the eye is sometimes a surprisingly good detector of sharp lines or a sharp cut-off in the spectrum of a random signal, it might be quite insensitive to changes through which the spectrum remains relatively smooth.

The velocity probe has the same size and shape as the temperature probe and is very sensitive to plankton effects because a change in the boundary-layer thickness over the film produces a d.c. shift in the indicated mean velocity. The record from this instrument shows many spikes from particles which strike the probe or come very close to it and occasional steps which indicate that there is something lodged on the probe tip. Most of these fall off within a few seconds but a few persist and the probe has to be 'washed' with a jet of water directed over the film against the mean flow.

It has been our practice to wash both probes whenever the velocity probe becomes dirty. If it is assumed that the intervals of time between the incidence of particles which stick to the probes are governed by a Poisson distribution and that such events at the two probes are statistically independent, it can be shown that the temperature probe can be expected to be clean 70 % of the time.

Unfortunately we do not know how seriously the spectrum might be affected in samples drawn from periods when the probe is dirty. About all that we can say

is that fouling should only reduce the sensitivity at high frequencies and that any spectra which appear unusually low at high frequencies might be viewed with some suspicion on this account. Thus far we have not seen any spectra which we could confidently ignore for this reason so it is possible that the effects are not important.

For a typical probe the temperature sensitivity of the complete system has been determined at 52 V/degC at full gain. With this sensitivity the range of temperature over which the system does not require re-balancing is  $\pm 17.7$  degC and  $\pm 0.028$  degC for the surface unit at minimum and maximum gain respectively. The overall noise level is equivalent to an r.m.s. fluctuation of  $1.7 \times 10^{-4}$  degC in the band 0.01 Hz to 1 kHz.

### 3. Spectral analysis

The continuous temperature and velocity records are scanned visually to select samples to be analysed. The main requirements for a satisfactory sample are that it be at least 90 sec long, that the signal level be approximately statistically constant, and that it contain no overloads, gain changes, probe washes, large changes in ship speed, or other disasters. In addition to these conditions it is necessary that both the velocity and temperature signals be large with respect to the instrumental noise level and that all gains be set at a suitable level to yield records well above tape noise. Gain settings are often far from optimum because it is difficult to predict the signal level in advance. When all of these conditions are taken into account we have only a very small number of satisfactory samples in many hours of records.

About half of the power spectra were calculated with the analogue equipment described by GSM and the remainder were done digitally on a Raytheon 250 computer. Because we are interested in power spectra over a large range of eddy sizes (about  $4\frac{1}{2}$  decades) we have broken each digital spectrum calculation into six sections. This is done with six low-pass constant delay analogue filters with cut-off frequencies spaced approximately equally on a logarithmic scale from 2 Hz to 1 kHz. The redundancy of some of the spectral outputs resulting from the use of this method, coupled with the multiplicity of recordings of the same signal, provides a useful consistency check on the final spectrum. Several spectra were computed by both digital and analogue methods and no large differences were found.

### 4. Experimental results and discussion

Velocity and temperature spectra were calculated for twelve samples and six pairs of spectra are shown in figures 6–11. The first three were obtained from data recorded in the Cape Mudge area in August 1962 and the other three are from the open sea in November 1962. Of these, figures 9 and 10 are the result of analogue computations and the remainder are from digital calculations with every third point from the computer output plotted to illustrate the scatter of the points, yet avoid overcrowding.

These six runs were chosen as representative of the twelve and include two 'good' runs from each area and two which will be used to illustrate some features of the observations which are not easy to interpret. Particulars of all twelve runs are given in table 1.

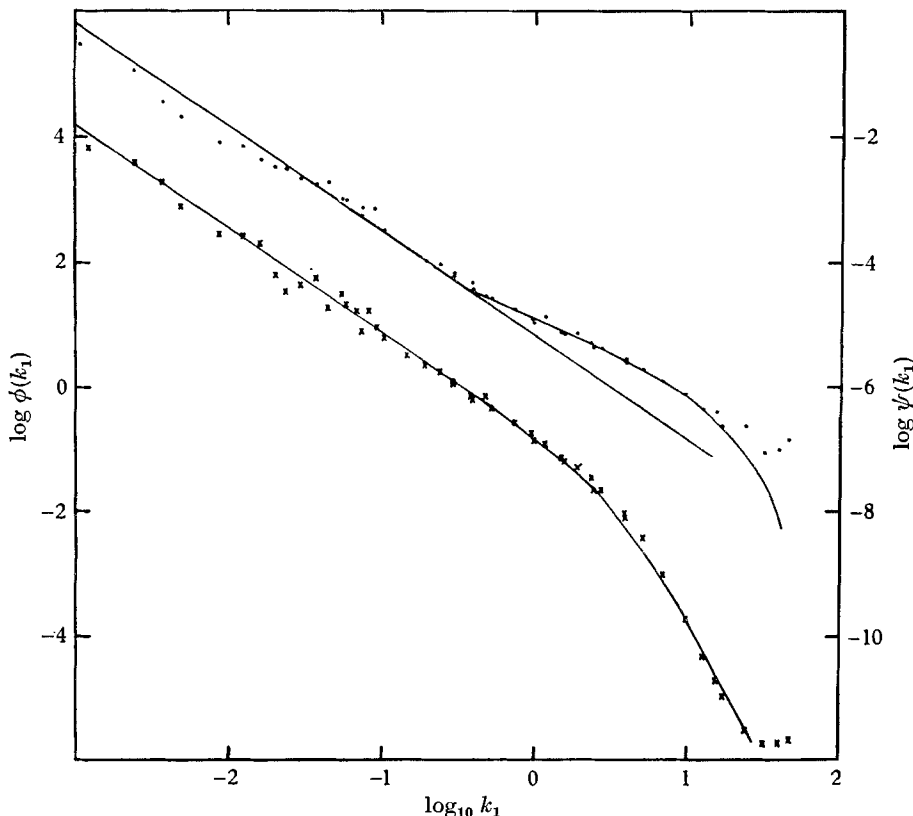


FIGURE 6. Temperature and velocity spectra from run 1, a sample recorded at a depth of 23 m near Cape Mudge, Discovery Passage. ( $\bullet$ ),  $\psi(k)$ , (degC)<sup>2</sup>/unit wave-number; ( $\times$ ),  $\phi(k)$ , (cm/sec)<sup>2</sup>/unit wave-number.

In the case of the temperature spectra, Batchelor's curve has been fitted to the 'viscous-convective subrange' by translations along both axes, rotation being prohibited. We have felt free to do this because the value of  $\gamma$  is not accurately known and the spectra do not extend to high enough wave numbers to permit the determination of  $\chi$  by equation (7). Equation (5) is fitted to the low wave-number end of the data, giving somewhat reduced weight to the extreme low wave-number points since the accuracy of both the observations and the analysis decreases there. The most obvious characteristic of the temperature spectra is that they all have regions in which the slope on the log plot is very close to  $-1$  and in fact they all agree with Batchelor's curve over a considerable range when that curve is fitted by the method described above. This is inconsistent with the spectrum proposed by Pao, so if the cascading rate hypothesis is to have any merit, it must depend on more than just  $\epsilon$  and  $k$ .

Run no.	Time	Sample length (sec)	Depth (m)	Towing speed (cm/sec)	Water temp. (°C)	$q$	$k_*/k_s$	$\epsilon$ (cm <sup>2</sup> sec <sup>-3</sup> )	$\beta_1$	$\chi$ (degC <sup>2</sup> sec <sup>-1</sup> )
1	15.29/20/8/62	175	23	127	9.8	3.6	$2.0 \times 10^{-2}$	$1.7 \times 10^{-1}$	0.28	$1.2 \times 10^{-6}$
2	09.46/21/8/62	380	15	131	9.8	4.6	$2.3 \times 10^{-2}$	$5.2 \times 10^{-1}$	0.31	$4.2 \times 10^{-4}$
3	10.03/21/8/62	390	15	163	9.8	3.0	$2.7 \times 10^{-2}$	$3.3 \times 10^{-1}$	0.34	$5.2 \times 10^{-4}$
4	10.52/21/8/62	240	15	146	9.8	1.7	$2.0 \times 10^{-2}$	$1.3 \times 10^{-1}$	0.40	$9.7 \times 10^{-6}$
5	15.13/21/8/62	100	23	126	9.8	0.72	$4.3 \times 10^{-2}$	$1.7 \times 10^{-1}$	0.47	$2.9 \times 10^{-6}$
6	13.31/19/11/62	160	90	140	7.9	5.0	$1.7 \times 10^{-2}$	$4.4 \times 10^{-4}$	0.25	$3.2 \times 10^{-7}$
7	10.41/23/11/62	508	27	115	11.0	7.2	$1.9 \times 10^{-2}$	$5.2 \times 10^{-3}$	0.27	$5.7 \times 10^{-7}$
8	11.36/23/11/62	468	15	100	11.0	2.4	$3.3 \times 10^{-2}$	$2.5 \times 10^{-2}$	0.39	$5.6 \times 10^{-7}$
9	12.36/23/11/62	150	58	125	8.7	10.9	$7.2 \times 10^{-3}$	$4.8 \times 10^{-3}$	0.14	$4.3 \times 10^{-6}$
10	17.15/23/11/62	246	89	125	7.9	13.2	$6.5 \times 10^{-3}$	$1.1 \times 10^{-3}$	0.13	$1.6 \times 10^{-7}$
11	18.26/23/11/62	294	89	121	8.2	4.2	$1.7 \times 10^{-2}$	$4.8 \times 10^{-4}$	0.25	$7.2 \times 10^{-8}$
12	18.36/23/11/62	190	89	128	8.2	3.3	$1.9 \times 10^{-2}$	$1.0 \times 10^{-3}$	0.27	$1.3 \times 10^{-7}$

TABLE 1

Before trying to estimate the constants describing the temperature spectra we must examine the validity of the velocity spectra. In all cases we have attempted to fit a curve representing the function  $\epsilon^{1/2} \nu^{1/2} F(k_1/k_s)$ , where  $F(k_1/k_s)$  is

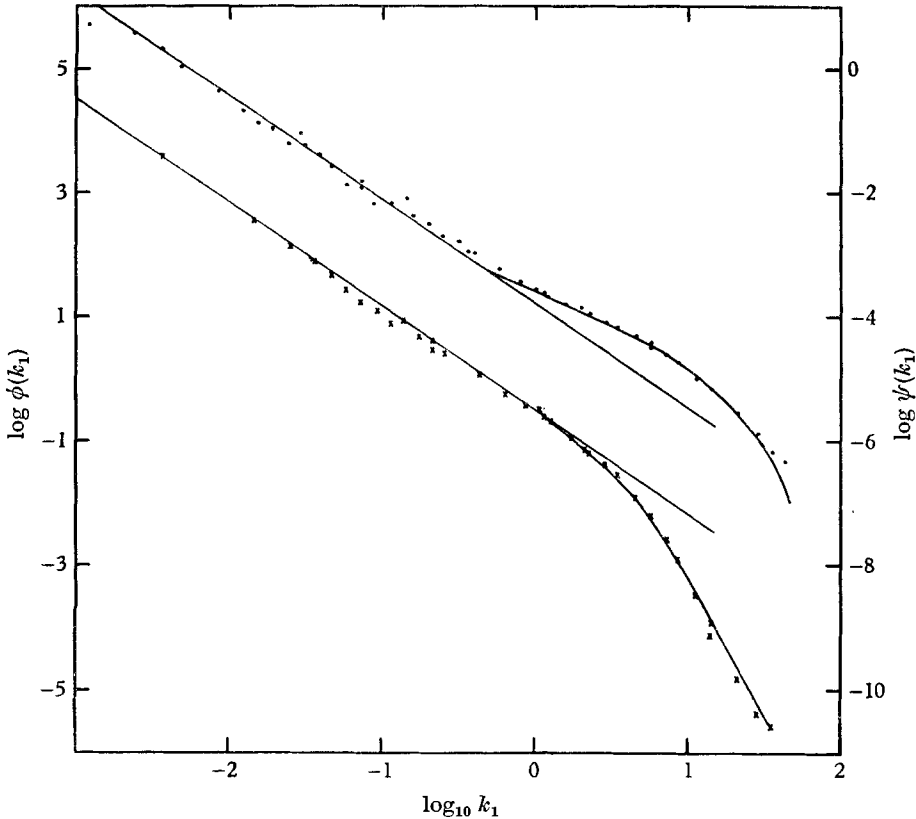


FIGURE 7. Temperature and velocity spectra from run 2, at a depth of 15 m near Cape Mudge.

the 'universal function' based upon the observations of GSM and described by Stewart & Grant (1962). In several cases (e.g. figures 8 and 11) the fit is not good. We find it hard to believe that the 'universal curve' can be very far wrong as a description of high-Reynolds-number locally isotropic turbulence because, since it was published, it has received very strong support from two entirely independent measurements in air (Pond, Stewart & Burling 1963; Gibson, M. M. 1963), and because we made a series of measurements in Discovery Passage in November 1963, using a new bridge, and obtained spectra in very good agreement with GSM. It is unlikely that faulty equipment was to blame because the inshore and offshore data were obtained with different bridges, both of which performed satisfactorily in all laboratory calibrations.

We therefore conclude that either the turbulence meter was detecting temperature fluctuations, or that we were not observing high-Reynolds-number locally isotropic turbulence, or both. Run 4 (figure 8) is an example of a velocity

spectrum in which either or both of these phenomena might have occurred. We know the sensitivity of the velocity bridge to low-frequency changes in temperature, but this does not apply at high frequencies. Because of the feedback in the

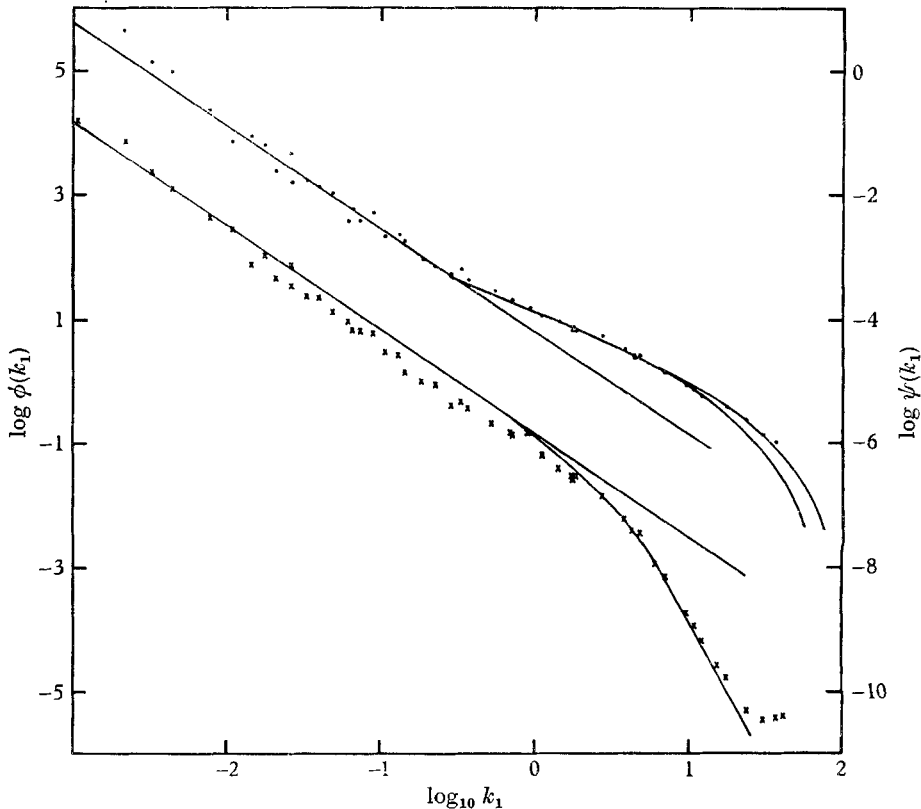


FIGURE 8. Temperature and velocity spectra from run 4, at a depth of 15 m near Cape Mudge.

bridge and the use of linearizing circuits, Fabula's method of measuring frequency response is unsuitable. The velocity spectrum in run 3 (not shown) has a similar appearance but with smaller departures from the 'universal curve'. For all wave-numbers greater than unity, the ratio  $\psi(k)/\phi(k)$  is the same for these two pairs of spectra. This suggests that the velocity bridge was observing temperature fluctuations; but on the other hand this ratio is ten times as large in run 9 (not shown) and a very careful check of the records produced no evidence that would suggest any mistake such as an incorrectly recorded gain in that run. If we were to conclude that the velocity spectra in runs 3 and 4 are affected by temperature we would also have to regard as fortuitous the fact that the spectra have the same slope at high wave-number as the 'universal curve'. Thus it seems unlikely that temperature fluctuations gave rise to the anomalous velocity spectra in runs 3 and 4.

At the time that the data of run 4 were recorded the ship was trapped in what is locally known as a 'tide line'. This is a common phenomenon in waters with

strong tidal currents. There is a line of foam, seaweed and driftwood on the surface indicating a surface convergence and a considerable shear across the line, often amounting to more than 100 cm/sec in one or two metres. At the southern end of

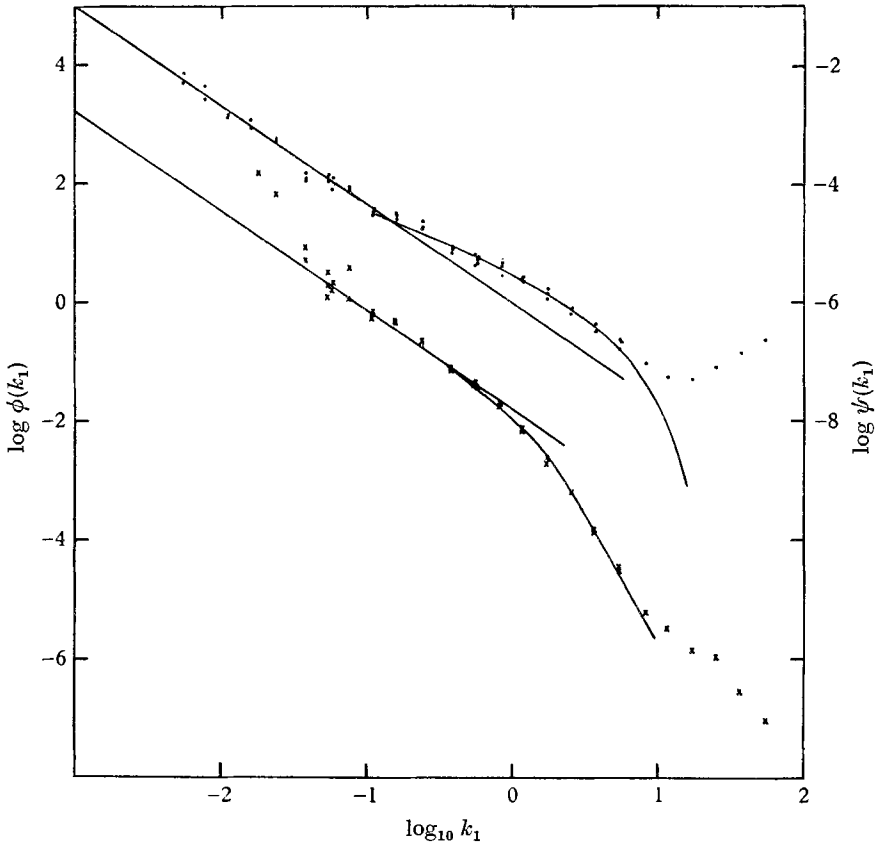


FIGURE 9. Temperature and velocity spectra from run 7 at a depth of 27 m in the open sea.

Discovery Passage, a tide line of this type exists at the edge of the separated flow behind Cape Mudge on the south-going tide. Because of the surface convergence, a slowly moving ship tends to fall into the line, and when this happens it may be necessary to use a speed of about six knots with respect to the water to gain sufficient steerage way to turn her bow out of it. The probes were at a depth of 23 m and the shear surface need not be vertical, but nevertheless it is possible that this persistent organized shear could generate turbulence on scales much smaller than the depth of the water and that this could appear in the spectrum as a peak at quite high wave-numbers. The records make no mention of a tide line at the time of run 3 and the ship's track suggests that at the time she was well clear of the separation behind Cape Mudge.

In run 10 (figure 11) we have another velocity spectrum with large departures from the 'universal curve'. In this case the ratio  $\psi(k)/\phi(k)$  is small enough that the temperature sensitivity seems unlikely to be involved but the assumption of

locally isotropic turbulence is open to doubt. The data were recorded while the submarine was passing through a patch of turbulence in the thermocline at a depth of 90 m. There is considerable evidence to suggest that, although such

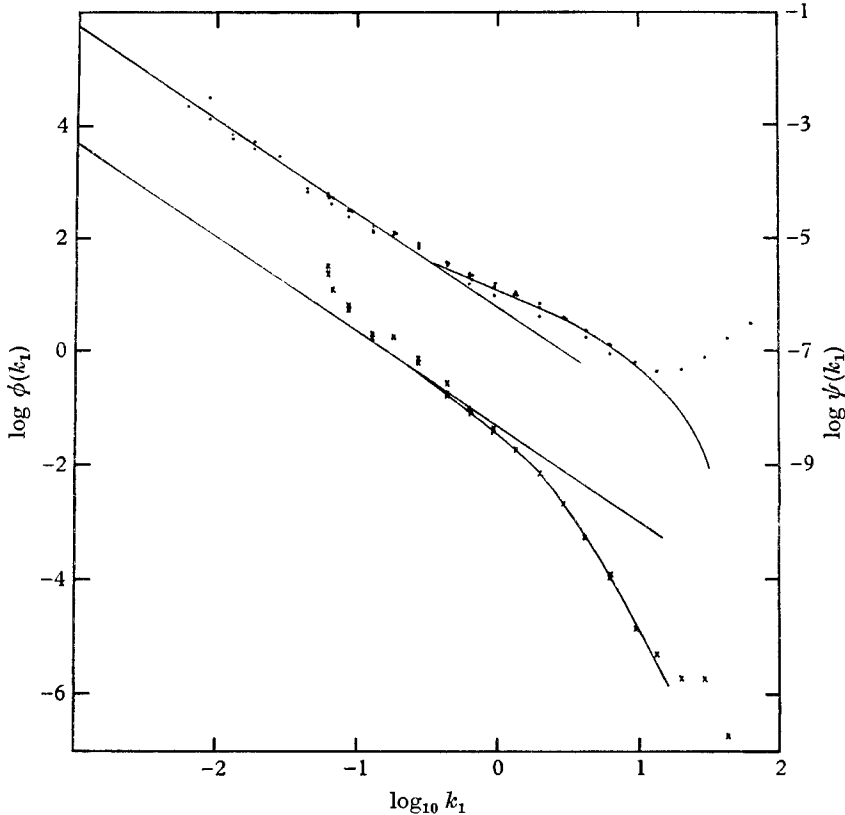


FIGURE 10. Temperature and velocity spectra from run 8 at a depth of 15 m in the open sea.

patches may have horizontal dimensions of tens or hundreds of metres, the typical vertical extent may be only of the order of 1 m. If this represents the scale of the shear which is giving rise to the turbulence one would not expect an extensive inertial subrange. The four points at very low wave-numbers are probably due to surface wave motion rather than turbulence. The velocity spectrum in run 9 has similar characteristics, and it will be seen below that the corresponding temperature spectra have peculiar features.

Clearly these questions can only be resolved by further observations designed with these problems in mind. In the meantime, the temperature spectra given here appear to be valid and the reader will have to interpret the supporting velocity spectra (particularly runs 3, 4, 9 and 10) with some caution.

The rate of energy dissipation,  $\epsilon$ , has been determined by the method described by Stewart & Grant (1962) for 'noisy' spectra except that in the four runs where there is reason to suspect low-Reynolds-number effects (e.g. figures 8 and 11) we have fitted the universal curve at the high wave-number end and allowed some points to fall below the curve.



Given adequate spectral measurements, one would like to determine  $\chi$  from (7),  $\epsilon$  from the velocity spectrum and then determine the two constants  $\beta_1$  and  $q$ . The temperature spectra shown above are obviously affected by noise at large

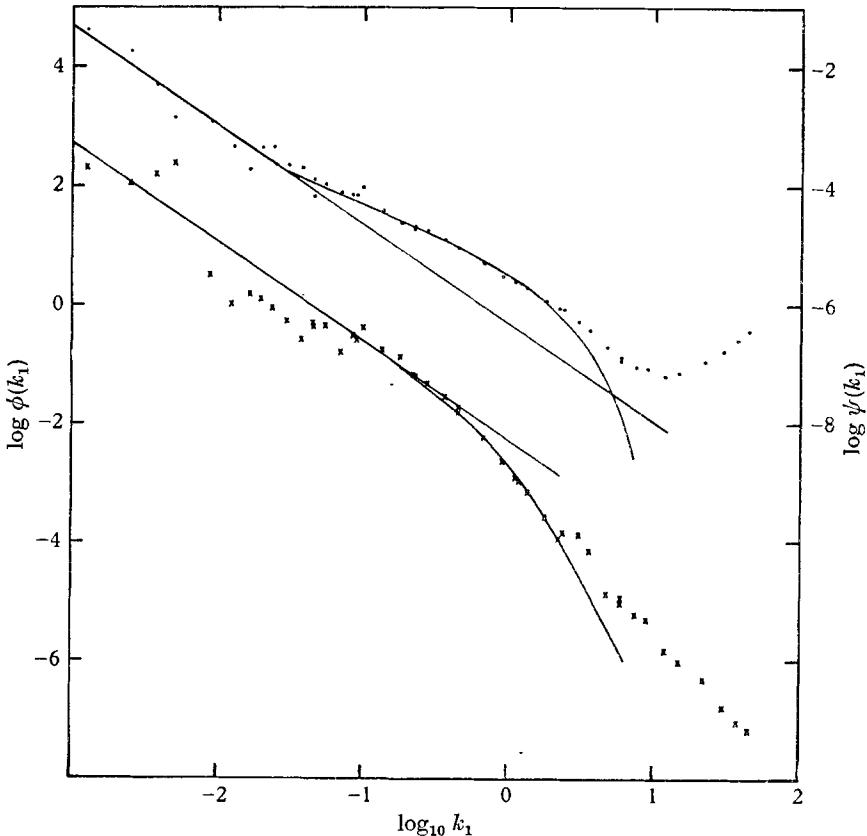


FIGURE 11. Temperature and velocity spectra from run 10 at depth of 89 m in the open sea.

wave-numbers and it is not possible to determine the integral in (7). The quantity  $k_*$  does appear to be well defined, and it is small enough that (6) can be used to represent the viscous convective subrange in the vicinity of  $k_*$ . Combining (4) and (6) we have

$$k_*/k_s = (\beta_1/q)^{\frac{2}{3}}, \tag{9}$$

a universal constant.

Values of  $k_*/k_s$  are given in table 1 for all runs. The average value is  $2.1 \times 10^{-2}$ , which is surprisingly low, but the data of Gibson & Schwartz support a value of this order. The large scatter among our individual values does not appear to us to be the result of random experimental errors and suggests the possibility that the assumptions on which Batchelor's theory is based may be invalid for some of these runs. In this respect we have already expressed our doubts about the scale at which the turbulence may have been generated in runs 9 and 10 and these yield values of  $k_*/k_s$  which differ from the mean of the other runs by a

factor of 3.5. Our best estimate of  $k_*/k_s$  is the average of all runs except 9 and 10, and this is  $2.4 \times 10^{-2}$  with a standard deviation of  $0.8 \times 10^{-2}$ .

In the viscous-convective range we have fitted equation (5). This is done by plotting

$$G(B) = \left\{ \Phi(B)/B - \int_B^\infty \Phi(y) dy \right\}$$

to the same scale as the spectrum on translucent paper, overlaying the two plots, and adjusting them in two dimensions for best fit. The line  $B = 1$  on the  $G(B)$  plot corresponds to the value  $k'_B = k_B/(2q)^{1/2}$  on the spectrum plot. Since  $k_B = k_s(\nu/D)^{1/2}$  and  $k_s$  is determined from the velocity spectrum,  $q$  is given by

$$q = \frac{1}{2}(k_s/k'_B)^2(\nu/D).$$

The part of the viscous convective range which appears in our measured spectra is only slightly curved and most of the curvature is out in the range where the data are beginning to be affected by noise. The result is that we find this curve-fitting procedure to be a very insensitive way to measure  $q$ . In fitting the curves we have allowed very few points to fall below the line, particularly at the high wave-number end, because of the probability of the signals being affected by noise. In figure 8 we have drawn two curves. The one on the left obeys the above rule and yields  $q = 1.7$ . With a little more faith in the data at large wave-numbers we could fit the other curve, which would give  $q = 0.9$ . The deficiency lies in the quality of the data rather than the method so we have given our best estimates of  $q$  in table 1. Once again runs 9 and 10 give odd results and we feel justified in leaving them out of our average. Run 5 had a rather high noise level and a shorter than usual portion of the spectrum appears to be noise free. This means that it departs less from a straight line than the others and there is more uncertainty in  $q$ , although the value given in the table results from the rule that we make the best fit without letting points fall below the line.

If we leave out these three runs the average value of  $q$  is  $3.9 \pm 1.5$ . Batchelor & Townsend (1956) have concluded from observation of velocity derivatives that  $q \approx 2$ , and Reid (1955) gives a theoretical argument which suggests that  $q \approx 2.5$ . Recently, Gibson (1966) has argued that the definition of  $\gamma$  requires that  $q$  lie between the limits  $\sqrt{3} < q < 2\sqrt{3}$ . Our result lies near the upper limit of this range but it is very difficult to estimate the probable error. Systematic errors could easily arise through various causes: the difficulty of curve fitting, possible effects of dirt on the probe, smearing of the very short-scale temperature structure by the mean flow gradients around the probe tip, inaccurate scaling of the constants used in the frequency response correction (see Fabula 1968). It has been pointed out above that the probe can be expected to be dirty about 30% of the time and a small loss of response at high frequencies would lead to an abnormally high value of  $q$ . Since the average time between washes is long compared with the length of a run we can estimate the probability that the probe is dirty during a run by ignoring the possibility of dirt arriving on the probe within the time period of the run. With this assumption it is easy to calculate the probability that the probe will be dirty during any given number of runs out of a sample of nine. The

result is that the probability of  $x$  dirty runs, when  $x$  takes the values 0 to 6, is, in order, 0.04, 0.16, 0.27, 0.27, 0.17, 0.07, 0.02.

Values for  $\beta_1$  can be calculated from (9), which may be written

$$\beta_1 = q(k_*/k_s)^{\frac{2}{3}},$$

and the results are given in table 1. The average of all runs except 5, 9 and 10 is 0.31 and the standard deviation is 0.06.

The final column in table 1 gives values of  $\chi$  determined from (4) with  $\beta = 0.31$ . These are discussed by Grant *et al.* (1968) in terms of the oceanographic situation prevailing at the time.

## 5. Conclusion

It is clear from these experiments that the temperature spectrum rises above the  $k^{-\frac{5}{3}}$  line at high wave-numbers and that the data in this region can be fitted by a curve of the shape predicted by Batchelor (1959). In order to make this fit, however, we have not insisted that  $q$  and  $k_*/k_s$  behave as absolute constants. This does not necessarily mean that Batchelor's theory is wrong or inaccurate because we cannot be certain that the assumptions of his theory are appropriate in all of the experiments and because our method of measuring  $q$  is very sensitive to experimental errors. If we disregard the runs that are most likely to be affected by small Reynolds number or experimental errors and assume that (4) and (5) are of the correct form, our best estimates of the constants in these equations are

$$k_*/k_s = 2.4 \times 10^{-2} \pm 0.8 \times 10^{-2}, \quad q = 3.9 \pm 1.5 \quad \text{and} \quad \beta_1 = 0.31 \pm 0.06.$$

The limits attached to these figures represent the standard deviation among the measurements.

This work was carried out over a period of several years and many people have made contributions to the work during this time. Mr R. W. Chappell was primarily responsible for the design of the resistance thermometer bridge and the recording system but we have frequently consulted Mr D. J. Evans, who has made significant contributions to the apparatus. The work would not have been possible without the study of frequency response of towed thermometers by Dr A. G. Fabula to which we have referred. We are grateful for the skilful and co-operative assistance of the captains and crews of the Royal Canadian Navy's research vessel *Oshawa* and the submarine H.M.C.S. *Grilse*. Personnel of the Pacific Oceanographic Group of the Fisheries Research Board of Canada made the measurements of temperature and salinity as a function of depth.

## REFERENCES

- BATCHELOR, G. K. 1959 *J. Fluid Mech.* **5**, 113.
- BATCHELOR, G. K. & TOWNSEND, A. A. 1956 Article in *Surveys in Mechanics*, p. 352. Cambridge University Press.
- CORRSIN, S. 1951 *J. Appl. Phys.* **22**, 469.
- FABULA, A. G. 1968 *J. Fluid Mech.* **33**, 449.
- GIBSON, C. H. 1966 *Institute for Radiation Physics and Aerodynamics*, University of California. Rep. no. IRPA-65-68.
- GIBSON, C. H. & SCHWARTZ, W. H. 1963 *J. Fluid Mech.* **16**, 365.
- GIBSON, M. M. 1963 *J. Fluid Mech.* **15**, 161.
- GRANT, H. L., MOILLIET, A. & VOGEL, W. M. 1968 *J. Fluid Mech.* **33**, 443.
- GRANT, H. L., STEWART, R. W. & MOILLIET, A. 1962 *J. Fluid Mech.* **12**, 241.
- NYE, J. O. & BRODKEY, R. S. 1967 *J. Fluid Mech.* **29**, 151.
- OBUKHOV, A. M. 1949 *Izv. Akad. Nauk SSSR, Geogr. i Geofiz.* **13**, 58.
- PAO, Y. H. 1965 *Phys. Fluids* **8**, 1063.
- POND, S., SMITH, S. D., HAMBLIN, P. F. & BURLING, R. W. 1966 *J. Atmospheric Sci.* **23**, 376.
- POND, S., STEWART, R. W. & BURLING, R. W. 1963 *J. Atmospheric Sci.* **20**, 319.
- REID, W. H. 1955 *Proc. Camb. Phil. Soc.* **51**, 350.
- STEWART, R. W. & GRANT, H. L. 1962 *J. Geophys. Res.* **67**, 3177.